Lung Damage Assessment from Exposure to Pulsed-Wave Ultrasound in the Rabbit, Mouse, and Pig

William D. O'Brien, Jr., *Fellow, IEEE,* and James F. Zachary

***Abstract*—The principal motivation of the study was to assess experimentally the question: "Is the *MI* (Mechanical Index) an equivalent or better indicator of nonthermal bioeffect risk than $I_{SPPA.3}$ (derated spatial peak, pulse average intensity)?". To evaluate this question, the experimental design consisted of a reproducible biological effect in order to provide a quantitative assessment of the effect. The specific biological effect used was lung damage and the species chosen was the rabbit. This work was initiated, in part, by a study [1] in which lung hemorrhage was observed in 7-week old C3H mice for diagnostic-type, pulsed-wave ultrasound exposures, and, therefore, 6- to 7-week old C3H mice were used in this study as positive controls. Forty-seven adult New Zealand White male rabbits were exposed to a wide range of ultrasound amplitude conditions at center frequencies of 3 and 6 MHz with all temporal exposure variables held constant. A calibrated, commercial diagnostic ultrasound system was used as the ultrasound source with output levels exceeding, in some cases, permissible FDA levels. The *MI* was shown to be at least an equivalent, and in some cases, a better indicator of rabbit lung damage than either the $I_{SPPA.3}$ or $p_{r.3}$ (derated peak rarefactional pressure), thus answering the posed question positively. Further, *in situ* exposure conditions were estimated at the lung pleural surface (PS); the estimated *in situ* $I_{SPPA.PS}$ and $p_{r.PS}$ exposure conditions tracked lung damage no better than $I_{SPPA.3}$ and $p_{r.3}$, respectively, whereas the estimated *in situ* MI_{PS} exposure condition was a slightly poorer predictor of lung damage than *MI*. Finally, the lungs of six adult crossbred pigs were exposed at the highest amplitude exposure levels permittted by the diagnostic ultrasound system (to prevent probe damage) at both frequencies; no lung damage was observed which suggests the possibility of a species dependency biological effect.**

I. Introduction

When the US Food and Drug Administration initiated the regulation of diagnostic ultrasound equipment in the mid-1980s [2], it set application-specific intensity limits which manufacturers could not exceed. These limits were (and are) *not* based on safety considerations but rather on the known maximum output limits of diagnostic ultrasound equipment at the time when the Medical Devices Amendments were enacted, in May 1976, hence the phrase *pre-amendments levels*. In the late 1980s, an activity was initiated to develop a diagnostic ultrasound equipment standard which had, as its basis, biophysical indicators which would provide to equipment operators during a diagnostic procedure a means of assessing the potential risk from either a thermal or a mechanical ultrasound bioeffect. The approval of the *Standard for Real-Time Display of Thermal and Mechanical Indices on Diagnostic Ultrasound Equipment* [3], commonly referred to as the Output Display Standard (ODS), gave manufacturers a standardized procedure to provide on diagnostic ultrasound equipment either a Thermal Index or Mechanical Index [3]–[5].

The purpose of developing the the ODS was to provide the capability for users of diagnostic ultrasound equipment to operate their diagnostic ultrasound system at levels higher than had been possible under the application-specific limits in order to have the potential for greater diagnostic capabilities. In doing so, the possibility existed for the potential to do harm to the patient. Thus it becomes imperative to provide to the equipment operators a means for assessing the system's output and specifically a means for assessing the biological consequences of that increased output. The ODS does this, in part, by providing calculated quantities which are based on biophysical indicators, *viz.*, an index which relates to the maximum tissue temperature increase in the beam (the Thermal Index) and an index which relates to the potential for producing cavitation (the Mechanical Index). These two biophysical indices were provided so that the equipment operator would have real-time information available to make appropriate clinical decisions, *viz.*, benefit *vs.* risk, and to implement the ALARA (As Low As Reasonably Achievable) principle [6].

The production of heat in biological tissues from diagnostic ultrasound has received considerable attention in the past few years [7]–[8]. While there are still important issues to be resolved regarding the relation between actual tissue temperature increase and the Thermal Indices, there is a greater degree of understanding here than with that of the Mechanical Index which is intended to represent the potential for cavitation in tissue, although there has never been a reported case where cavitation has been known to occur from scanning a patient with diagnostic ultrasound equipment.

Manuscript received May 2, 1996; accepted September 4, 1996. This work was supported in part by Advanced Technology Laboratories, Bothell, WA.

W. D. O'Brien is with the Bioacoustics Research Laboratory, Department of Electrical and Computer Engineering, Beckman Institute for Advanced Science and Technology, University of Illinois, 405 North Mathews Urbana, IL 61801 (e-mail: wdo@uiuc.edu).

J. F. Zachary is with the Division of Pathology, Department of Veterinary Pathobiology, University of Illinois, 2001 South Lincoln Avenue, Urbana, IL 61801.

The application-specific regulatory procedures [2] have maximum regulatory limits for the derated spatial peak, pulse average intensity ($I_{\mathrm{SPPA.3}}$) which are thought to provide a measure of safety for the production of cavitation, although it has never been demonstrated that $I_{\mathrm{SPPA.3}}$ is directly related, in an exposure-effect context, to the production of cavitation in biological tissues. The *MI*'s purpose was to provide a biophysical indicator for the production of cavitation, hence the development of the ODS [3].

This contribution provides the first *in vivo* bioeffect report which examines whether the ODS's Mechanical Index is an appropriate exposure-effect quantity, and examines not only the *MI*'s exposure-effect relationship but also the $p_{\mathrm{r.3}}$'s and $I_{\mathrm{SPPA.3}}$'s exposure-effect relationship in this regard. The development of the Mechanical Index was based on theoretical and *in vitro* experimentation by investigators [9]–[10] who discovered a simple relationship between acoustic pressure and the onset of cavitation under an assumption that the optimum bubble size is present. The theory assumed isothermal growth, adiabatic collapse, an incompressible host fluid, and neglected gas diffusion into the bubble and the experiments were conducted in an aqueous medium, not tissue. These *in vitro* observations were the basis for the adoption of the ODS [3] which defined the Mechanical Index, *MI*, as

$$MI = \frac{p_{r.3}}{\sqrt{f}} \tag{1}$$

where $p_{\mathrm{r.3}}$ is the derated (the "0.3" subscript denotes the numerical value of the derating factor of 0.3 dB/cm-MHz) peak rarefactional pressure (in MPa) and f is the ultrasonic center frequency (in MHz).

In regard to *in vivo* studies which have addressed the presence of cavitation-like phenomenon, it was demonstrated that ultrasonically induced bubble-like activity can result in lung damage in adult mice [1]. (Ill-defined terms like *cavitation-like*, *bubble-like*, and *bubble-related*, for example, are used because it has not been determined what the mechanism is that induces ultrasound damage in lung tissue; what appears to be required is gas bodies in tissue to elicit effects [11].) Their threshold observations correlated well with the frequency-dependent, *in vitro* cavitation experiments [12]–[13]. Although the special environment of tissues (and lungs) was not considered in the formulation of *MI*, it was thought to have the potential to be a useful predictor of bubble-related effects in tissues, an issue which is evaluated by the study reported herein.

The study design was based on assessing whether the *MI* was an equivalent or better predictor of a mechanical bioeffect than $I_{\mathrm{SPPA.3}}$, one of the quantities regulated by FDA [2]. Two center frequencies were used because the *MI* definition (1) takes into account a possible frequency dependency. Further, the experimental design consisted of a biological effect that was reproducible in order to provide a quantitative assessment of the effect under superthreshold exposure conditions to determine appropriate exposure-effect response relationships.

II. Animal Procedures

Five to 5 1/2-month-old (8 to 9 lb) New Zealand White male rabbits were obtained from Myrtle's Rabbitry, Inc. (Thompson Station, TN) and ultrasound exposures were performed within 5 days of the time of shipment receipt. Six to 7-week-old C3H male mice were obtained from Harlen Sprague Dawley Laboratories (Indianapolis, IN) and ultrasound exposures were performed within 1 week of the time of each shipment receipt. Ten to 12-week-old (60 to 70 lb) crossbred pigs were obtained from the University of Illinois College of Veterinary Medicine swine breeding farm (Urbana, IL) and ultrasound exposures were performed within 2 days of the time of shipment receipt.

Animals were observed to be free of clinical signs suggestive of respiratory disease by visual inspection before the start of the studies and were confirmed to be free of respiratory disease at postmortem examination. Animals were provided housing, food, and veterinary care according to University of Illinois and NIH guidelines.

Rabbits were anesthetized with a combination of ketamine hydrochloride (Ketamine®) (35.0 mg/kg) and xylazine (Rompun®) (5.0 mg/kg) administered subcutaneously. Mice were anesthetized with a combination of ketamine hydrochloride (Ketamine®) (125 mg/kg) and xylazine (Rompun®) (25 mg/kg) administered intraperitoneally. Pigs were anesthetized with a combination of ketamine hydrochloride (Ketamine®) (5.0 mg/kg), xylazine (Rompun®) (5.0 mg/kg) and Telazol® (10 mg/kg) administered intermuscularly.

For each animal, the skin around the left lateral side was clipped with an electric shaver and the hair removed with a depilatory agent (Neet® or Nair®) to maximize sound transmission. The anesthetized animal was placed on its right side with the left lateral side upward. The left lateral side of the animal was in direct contact (using a commercial coupling agent) with the ultrasound transducer. The transducer was firmly supported by clamps connected to a solid supporting structure, and the ultrasound image was directed between the ribs (intercostal space) so that the ultrasound beam's focus was on the pleural surface of the left lobe (mice) or the left caudal lobe (rabbits and pigs). Verification that the ultrasound beam was directed toward lung parenchymal tissue was from the ultrasound image with the system operating at very low acoustic pressure levels; higher acoustic pressure levels were used only to obtain the high-quality images shown in Fig. 1. The individuals preparing each animal for sonication (anesthetizing and depilating the animal, and positioning the commercial transducer) each were blinded to the exposure condition.

Animals were anesthetized and humanely killed by methods approved by the American Veterinary Medical Association, the University of Illinois Office of Laboratory Animal Care, and the University of Illinois Animal Care Committees. Mice were killed by exsanguination and decapitation; rabbits were killed with CO_2 and exsaguination; and pigs were killed with an overdose of barbituate and exsaguination. Lungs were handled gently and dis-

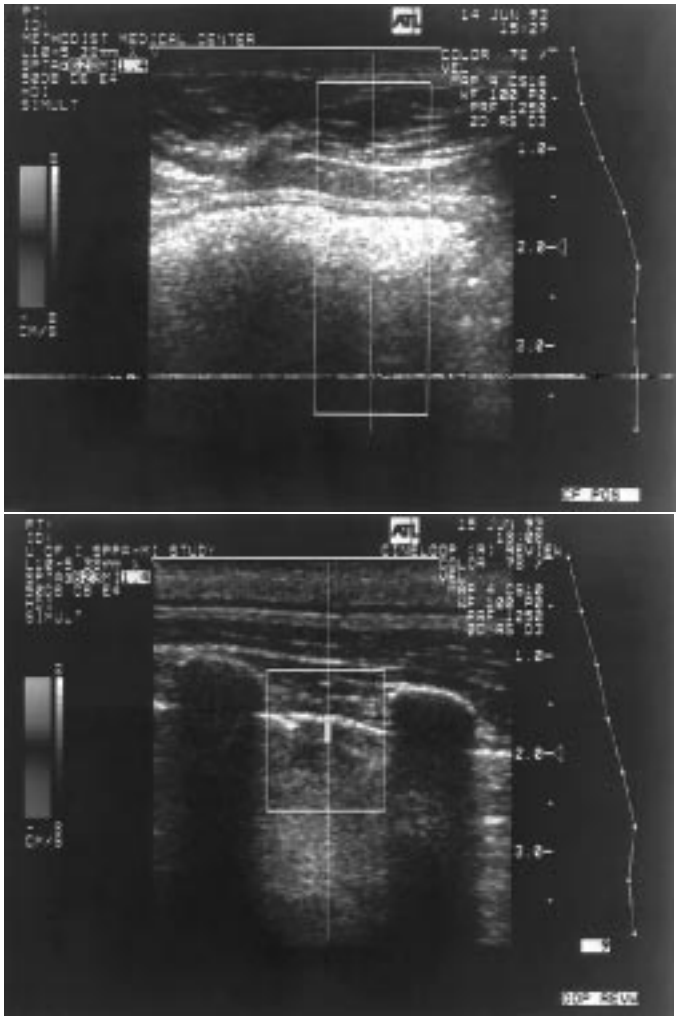

Fig. 1. Sonograms of (top) rabbit lung and (bottom) pig lung. Higher acoustic pressure levels were used only to obtain high-quality images.

sected free from the thoracic cavity and evaluated. The examiner was blinded to the exposure condition.

Evaluation of mouse lung included examination with a dissecting microscope. Rabbit and pig lungs were examined for surface hemorrhages and then sectioned in serial transverse planes to identify areas of hemorrhage in all lobes. For all animals, areas of hemorrhage were recorded in a semi-quantitative manner and in relative proportion to lung size on diagrams representing dorsal and ventral views of all lung lobes [14]–[15]. The degree of severity of hemorrhage in lung was indicated on these diagrams by varying the intensity of lead pencil shading (gray scale) of areas hemorrhage where little hemorrhage was shaded light gray and severe hemorrhage was shaded black. In preliminary studies, serial sections of sonicated lungs were examined macroscopically and microscopically in order to verify that the macroscopic interpretation of lung lesions as hemorrhage was, in fact, accurate.

The assignment of the numerical score to each lung (Table I) was based on clinical variables (survival, respiratory patterns, hemothorax, etc.) and macroscopic assessment of lung for hemorrhage. Lung hemorrhage was evaluated

TABLE I
QUANTITATIVE NUMERICAL CRITERIA FOR SCORING LUNG DAMAGE FOLLOWING SONICATION OF EACH ANIMAL (HISTOLOGIC EVALUATION REQUIRED TO CONFIRM THESE GROSS INTERPRETATIONS).

0	- normal lung, normal vital signs.
0.5	- equivocal hemorrhage, normal vital signs.
1	- minimal hemorrhage usually involving 1 to 4 foci measuring approximately < 5 mm in diameter, normal vital signs.
2	- mild hemorrhage that was greater in extent and severity than a score of 1.0, normal vital signs.
3	- moderate hemorrhage that was greater in extent and severity than a score of 2.0, normal vital signs.
4	- marked hemorrhage that was greater in extent and severity than a score of 3.0, abnormal vital signs.
5	- severe hemorrhage that was greater in extent and severity than a score of 4.0, abnormal vital signs, death.

Vital signs = Visual observation of the respiratory rate and breathing pattern during and after the period of ultrasound exposure.

qualitatively on the basis of color, location, and distribution (i.e., there was more intraparenchymal lung hemorrhage with a higher numerical score). Lungs with intraparenchymal hemorrhage were dark red-brown to black, and this color change was apparent throughout affected lung lobes. A score of 0 was assigned to lungs that had absolutely no hemorrhage; lungs with any or questionable (equivocal) foci of intraparenchymal hemorrhage no matter how small were assigned a score of 0.5 for consistency of scoring, animals with minimal intraparenchymal hemorrhage were assigned a score of 1, and so forth. Results are reported and analyzed in terms of the numerical criteria listed in Table I. Microscopic evaluation and characterization of lung lesions induced by pulsed-wave ultrasound have been described previously [16].

III. Exposimetry Procedures

The mice, rabbits, and pigs were exposed to ultrasound using one of the two transducers (ATL Model P3.5 at 3.0 MHz and ATL Model L10-5 at 6.0 MHz) connected to an Advanced Technology Laboratories (Bothell, WA) UM9 HDI® ultrasound imaging system (see Table II).

All animal experiments were conducted in the Laboratory Animal Care facility in the Veterinary Medicine Basic Sciences Building (VMBSB) at the University of Illinois. The ultrasound fields were calibrated prior to the study by the manufacturer. Following the 2-day study, on the following day, the HDI® system was transported from the VMBSB to the Bioacoustics Research Laboratory (BRL) at the University of Illinois for calibration. Also following the study, another set of calibrations was conducted at the manufacturer's headquarters with an HDI® system and identical probes, but different serial numbers. An ATL engineer was present during the animal experiments and controlled the HDI® output settings which,

TABLE II
OPERATING CONDITION QUANTITIES WITH THE ATL UM9 HDI® SYSTEM OPERATED IN TRIPLE MODE FOR THE TWO PROBES.

Quantities	P3.5 Probe	L10-5 Probe
Nominal focal depth	2 cm	2 cm
Echo center frequency	3.5 MHz	7.5 MHz
Scanned echo pulse cycles	1 cycle	2 cycles
Scanned echo pulse repetition frequency	607 Hz	335 Hz
Doppler drive frequency	3.0 MHz	6.0 MHz
Scanned Doppler pulse cycles	2 cycles	4 cycles
Scanned Doppler pulse repetition frequency	664 Hz	916 Hz
Static Doppler pulse cycles	3 cycles	6 cycles
Static Doppler pulse repetition frequency	1250 Hz	1250 Hz

for some of the exposure conditions, exceeded the normal FDA-allowable limits [2] which, for this clinical system was based on application-specific limits, the maximum of which was a derated spatial-peak, pulse-average intensity of 720 mW/cm^2, not an *MI* of 1.9 which was subsequently approved [5]. Table III summarizes the calibration values.

A. ATL Calibration Procedure

The probe was placed in a fixture and slightly submerged in water (degassed, deionized at 25°C) such that the ultrasound beam path was directed downward. The probe was able to be adjusted angularly across the sweep and nonscanned axes with micrometer controls. The GEC-Marconi PVDF Membrane hydrophone (Model Y-34-3598) was mounted submerged to a 3-D positioning system with 25 μm spatial accuracy. The hydrophone's signal was fed directly into a Tektronix DSA601A digitizing oscilloscope. Both the oscilloscope and hydrophone's positioning system were controlled by a MacIntosh Quadra 950 computer.

The ultrasound beam was aligned to be parallel with the vertical motion axis of the hydrophone positioner. Two depths (axial ranges) in the focal region separated by 2.5 cm were determined. The signal was maximized laterally across the beam at the nearer depth and angularly at the deeper depth. The positions were adjusted iteratively at both depths until the lateral adjustments were less than 100 μm. Beam centering was also checked at another intermediate depth to confirm alignment.

Prior to placing the probe in the water tank's fixture, the acoustic power was measured with a radiation force balance (RFB) system. The RFB system is tested weekly against an NIST transfer standard. At the same pulsing conditions used to measure the acoustic power with the RFB, and with the probe in the water tank's fixture, an axial scan (step size of 1 mm) was performed in the focal region. At each location the derated (at 0.3 dB/cm-MHz) temporal average intensity ($I_{\mathrm{TA.3}}$) was determined according to the Output Display Standard [3] procedures to locate the maximum value position of $I_{\mathrm{TA.3}}$ (the derated spatial peak temporal average intensity $I_{\mathrm{SPTA.3}}$ location). The hydrophone was then positioned at this axial position where a lateral scan was performed. The $I_{\mathrm{TA.3}}$ was determined in this lateral plane from which acoustic power was calculated. The hydrophone-determined acoustic power was then checked against the RFB-determined acoustic power to validate the hydrophone calibration.

The ultrasound system was put into static (nonscanned) pulsed Doppler mode. An axial scan (step size of 1 mm) was performed along the beam axis and at each location the derated (at 0.3 dB/cm-MHz) pulse average intensity ($I_{\mathrm{PA.3}}$) and Mechanical Index (*MI* - see(1)) were determined according to the Output Display Standard [3] procedures. The axial position at which the $I_{\mathrm{PA.3}}$ was a maximum was located and, at this location, the values of the derated spatial peak pulse average intensity ($I_{\mathrm{SPPA.3}}$) and *MI* were recorded.

B. BRL Calibration Procedure

The probe was sealed in an acoustically transparent cover because the probe had to be submerged in degassed water ($\approx$ 22°C) for the calibration procedure since the procedure required a horizontal-directed ultrasound beam path. Commercial coupling gel was used within the cover between the transducer surface and cover. The probe was clamped to the vernier positioners of the measurement tank to provide 3-D positional control and then submersed in the water tank. The GEC-Marconi PVDF Membrane hydrophone (Model Y-34-3598), a different hydrophone from that used by ATL, was connected to a 3-D computer-controlled positioning system which has an approximate 5 μm spatial accuracy. The loaded sensitivities for the Marconi hydrophone at 3 and 6 MHz were 0.0520 and 0.0559 μV/Pa, respectively, as determined from the UK National Physical Laboratory calibration report. The output from the Marconi hydrophone was connected to a digitizing oscilloscope (Tektronix Oscilloscope Model 11401 with Tektronix Amplifier 11A34) which was also controlled by the same computer (Tandy 4000 '386) as that of the 3-D positioning system.

A field survey of the hydrophone received signal from the ATL system operating in "triple mode" determined that the largest acoustic pressure level was from the pulsed Doppler mode signal. In "triple mode," three different pulse types are interleaved: a short echo pulse that is

TABLE III
SUMMARY OF CALIBRATION RESULTS OF THE DERATED (AT 0.3 DB/CM-MHZ) SPATIAL PEAK PULSE AVERAGE INTENSITY ($I_{SPPA.3}$), THE DERATED PEAK RAREFACTIONAL PRESSURE ($p_{r.3}$) AND THE MECHANICAL INDEX (MI) AND A SUMMARY OF THE ANIMALS EXPOSED FOR 5 MINUTES AT EACH OF THE EXPOSURE CONDITIONS; RABBIT NUMBERS IN PARENTHESES INDICATE THE NUMBER OF RABBITS USED IN THE INITIAL 18-ANIMAL STUDY.

Probe	Frequency (MHz)	$I_{SPPA.3}$ (W/cm^2)	$p_{r.3}$ (MPa)	MI	Mice	Rabbits	Pigs
P3.5	3	200	2.3	1.3		5 (5)	
P3.5	3	300	2.6	1.5		2 (2)	
P3.5	3	420	3.3	1.9		9	
P3.5	3	480	3.3	1.9			1
P3.5	3	510	3.3	1.9			1
P3.5	3	530	3.3	1.9			1
L10-5	6	200	2.0	0.8		5 (5)	
L10-5	6	510	2.9	1.2	2	10 (6)	
L10-5	6	1060	4.7	1.9		9	
L10-5	6	1310	5.4	2.2	1	3	2
L10-5	6	1480	5.6	2.3			1
Sham		0	0	0		4	

scanned for imaging purposes, a Doppler pulse that is scanned for color flow acquisition purposes, and a Doppler pulse that is static (nonscanned) for normal static Doppler acquisition purposes. The drive voltage to all three pulses is the same. Therefore, because of the transducer Q, the Doppler pulses (which have more cycles) achieve higher pressure amplitudes. For $I_{SPPA.3}$ and MI purposes, the pulse type with the highest I_{PA} and MI values was used.

Alignment of the beam axis perpendicular to the hydrophone's sensing element was accomplished by locating the maximum peak-to-peak hydrophone voltage at two lateral planes which were separated by 2 cm. Both planes were beyond the axial maximum. The angular positioning of the ATL probe was adjusted iteratively such that, when the hydrophone was moved from one plane to the other, no more than 200 μm readjustments were necessary in the lateral directions.

The focal point location was determined where the peak-to-peak hydrophone voltage was maximized along the beam axis. Axial scans were performed by scanning the hydrophone over a 1 to 2 cm distance (depending on the probe used) in increments of 500 μm and the received hydrophone voltage waveforms at each spatial increment were subsequently stored for off-line evaluation. The axial range of the hydrophone was determined by using the position cursors on the ATL system. The ATL system assumes a propagation speed of 1540 m/s. This distance was recalculated using the water's propagation speed of 1481 m/s.

The raw RF waveforms, each consisting of 2048 data points at 2 ns temporal spacings, were imported to a Sun Sparc2 to calculate the derated $I_{SPPA.3}$ and MI values as per the Output Display Standard procedures [3]. For the 3 and 6 MHz probes, the axial maximum locations were determined to be 1.47 and 1.39 cm, respectively.

C. Uncertainties

The uncertainties between the ATL and BRL exposure values were ±25% for $I_{SPPA.3}$ and ±13% for $p_{r.3}$ and MI. The values reported in Table III are the mean values of the ATL and BRL calibration values.

IV. Exposure Conditions

The study was initiated using four exposure conditions, *viz.*, two at a center frequency of 3 MHz ($I_{SPPA.3}$ = 200 W/cm^2 and MI = 1.3; $I_{SPPA.3}$ = 300 W/cm^2 and MI = 1.5) and two at a center frequency of 6 MHz ($I_{SPPA.3}$ = 200 W/cm^2 and MI = 0.8; $I_{SPPA.3}$ = 510 W/cm^2 and MI = 1.2). Eighteen rabbits were evaluated the first day after which the code was broken. There was no lung damage (score = 0; see Table I) in 10 of the rabbits, equivocal lung damage (score = 0.5) in four of the rabbits and minimal lung damage (score = 1) in four of the rabbits. The number of rabbits for each of these four exposure conditions are identified in Table III.

It was then judged necessary to increase the system's output level to the maximum extent achievable by the ATL HDI® system in order to increase the degree of lung damage since the hypothesis required that the study be conducted under superthreshold conditions. Table III lists the seven rabbit exposure conditions, all of which were 5 minutes in duration in order to assure superthreshold exposure conditions; this exposure duration was greater than the 3-minute exposure duration used by Child et al. [1], who found threshold levels in mice in the range of 0.7 MPa. In addition, while the hypothesis did not require sham exposures, because the level of lung damage was so minimal in rabbit lungs, it was decided after the initial 18 rabbits also

to include four sham exposed rabbits. Sixteen rabbits were exposed at 3 MHz, 27 rabbits at 6 MHz, and 4 rabbits were sham exposed. Also, three mice served as positive controls (also for a 5-minute exposure duration) because the rabbit lung damage was so minimal and because it had been reported [1] that the acoustic pressure levels being used were known to be above threshold levels for the production of lung hemorrhage in mice.

At the completion of the rabbit study, six pigs were exposed for a 5-minute duration at the highest possible acoustic pressure levels which could be achieved from the ATL HDI® system without damaging the probe. The purpose of the pig exposures was to evaluate whether or not lung damage could be produced at these high output levels. Three pigs were exposed at 3 MHz and three at 6 MHz.

V. Estimated *In Situ* Exposure Levels

The ATL HDI® imaging capability with its on-line electronic calipers was used to measure the distance to the pleural surface for all animals studied. All of the calibrations were performed using a derating factor of 0.3 dB/cm-MHz and these derated exposure values (see Table III) were based on the system's focus being located on the animal's pleural surface. The actual tissue attenuation of the interposed tissue between the animal's skin surface (where the probe was in contact) and the pleural surface was assumed to be greater than the 0.3 dB/cm-MHz derating factor. Therefore, a correction to this derating factor was used to estimate the *in situ* exposure levels at the pleural surface for each of the animals by assuming an attenuation coefficient of 1 dB/cm-MHz which was estimated from striated muscle attenuation coefficient values [17], that is,

$$p_{\mathrm{r.PS}} = p_{\mathrm{r.3}} 10^{\{(0.3-1.0)fd/20\}} \tag{2}$$

$$I_{\mathrm{SPPA.PS}} = I_{\mathrm{SPPA.3}} 10^{\{2(0.3-1.0)fd/20\}} \tag{3}$$

where $p_{\mathrm{r.PS}}$ and $I_{\mathrm{SPPA.PS}}$ are the estimated peak rarefactional pressure and spatial-peak, pulse-average intensity values at the pleural surface, respectively, f is the center frequency (in MHz) and d is the distance to the pleural surface (in cm). A modified Mechanical Index at the pleural surface was estimated from

$$MI_{\mathrm{PS}} = \frac{p_{\mathrm{r.PS}}}{\sqrt{f}} \tag{4}$$

VI. Statistical Analysis

The lung damage scores were statistically examined by three methods in order to provide an indication as to whether exposure-effect trends were evident. The intent is not to over analyze but rather provide different perspectives of the same data base. One approach placed the lung damage scores in exposure-based (different treatment) groups. The nonparametric Kruskal-Wallis Analysis of Variance (ANOVA) test was used because it could not be assumed that the population from which the samples under observation were normally distributed; this resulted from the arbitrary scoring criteria (see Table I) which was a quantitative means to indicate a qualitative finding, that is, the degree of lung damage. The Kruskal-Wallis ANOVA test was corrected for ties and was used to compare the medians of three or more unpaired groups. The Dunn's Multiple Comparisons post test, a variation of the Bonferroni test, was used to compare which medians were significantly different when the Kriskal-Wallis ANOVA test indicated significance ($p < 0.05$). The nonparametric Mann-Whitney U test was used to compare the the medians of two unpaired groups.

Spearman rank-order nonparametric correlation coefficient r_S was corrected for ties and quantifies the correlation between two paired samples of ranked data. This test also provides a p value which indicates the slope's significance relative to a zero slope and a 95% confidence interval of r_S which indicates 95% surity that the population value of the correlation coefficient lies within this interval.

Linear regression analysis was used to quantify the best-fit straight line between two variables; the correlation coefficient (r) described the amount of linear association and slope's p value indicated the slope's significance relative to a zero slope. The run test was used to evaluate whether the data deviated from the linear model where a run is defined as a series of consecutive points that are all above the linear regression line, or all below the linear regression line; if the raw data values are not related in a linear manner, the data points will tend to cluster in groups about or below the linear regression line resulting in a low number of runs and a low p value.

Statistical significance was at the 0.05 level, and all statistical calculations were performed using InStat® Macintosh Version 2.0 (GraphPad Software, San Diego, CA).

VII. Results

Table IV summarizes the lung damage score results in terms of their exposure values for both the 0.3 dB/cm-MHz derating ($I_{\mathrm{SPPA.3}}$, $p_{\mathrm{r.3}}$ and MI) and at the pleural surface ($I_{\mathrm{SPPA.PS}}$, $p_{\mathrm{r.PS}}$ and MI_{PS}; see (2)–(4)). The rabbit results are presented in terms of the eight exposure condition levels for $I_{\mathrm{SPPA.3}}$, $p_{\mathrm{r.3}}$ and MI, and the respective exposure condition values at the pleural surface for $I_{\mathrm{SPPA.PS}}$, $p_{\mathrm{r.PS}}$ and MI_{PS}. The individual results from the mouse and pig results are also listed.

Clinical signs were not observed in any animal exposed to pulsed-wave ultrasound.

Macroscopic lesions have been described previously [16]. Pulsed-wave ultrasound produced macroscopic hemorrhage in the lungs of mice and rabbits and no hemorrhage in the lungs of pigs. In mice, hemorrhage occurred in all lung lobes following exposure; in rabbits, hemorrhage occurred in pleura and subjacent lung that was contiguous with the ultrasound beam originating from the overlying transducer head.

TABLE IV

SUMMARY OF EXPOSURE (0.3 DB/CM-MHZ DERATED AND *in situ* PLEURAL SURFACE VALUES OF I_{SPPA}, p_r AND *MI*), DISTANCE TO PLEURAL SURFACE (d) AND LUNG DAMAGE SCORE (BASED ON CRITERIA LISTED IN TABLE I) FOR 47 RABBITS, 3 MICE AND 6 PIGS; FOR COMBINED RESULTS, THE LUNG DAMAGE SCORE VALUES ARE REPRESENTED AS THE MEAN ± STANDARD DEVIATION.

Frequency (MHz)	$I_{SPPA.3}$ (W/cm^2)	$p_{r.3}$ (MPa)	*MI*	$I_{SPPA.PS}$ (W/cm^2)	$p_{r.PS}$ (MPa)	MI_{PS}	d (mm)	Score	Count
Rabbit Results									
Sham	0	0	0	0	0	0	13 ± 1.0	0.13 ± 0.25	4
3	200	2.3	1.3	104 ± 10	1.7 ± 0.1	1.0 ± 0.04	14 ± 1.9	0.40 ± 0.55	5
6	200	2.0	0.8	64 ± 10	1.1 ± 0.09	0.5 ± 0.04	12 ± 1.7	0.20 ± 0.27	5
3	300	2.6	1.5	153 ± 10	1.9 ± 0.06	1.1 ± 0.04	14 ± 1.4	0.50 ± 0.71	2
3	420	3.3	1.9	220 ± 17	2.4 ± 0.09	1.4 ± 0.05	13 ± 1.6	0.56 ± 0.46	9
6	510	2.9	1.2	136 ± 20	1.5 ± 0.1	0.6 ± 0.04	14 ± 1.5	0.25 ± 0.35	10
6	1060	4.7	1.9	299 ± 51	2.5 ± 0.2	1.0 ± 0.09	13 ± 1.7	0.78 ± 0.44	9
6	1310	5.4	2.2	483 ± 27	3.3 ± 0.09	1.3 ± 0.04	10 ± 0.6	1.0 ± 0	3
Mouse Results									
6	510	2.9	1.2	420	2.6	1.1	2.0	2	1
6	510	2.9	1.2	420	2.6	1.1	2.0	3	1
6	1310	5.4	2.2	1080	4.9	2.0	2.0	3	1
Pig Results									
3	480	3.3	1.9	166	1.9	1.1	22	0	1
3	510	3.3	1.9	158	1.8	1.1	24	0	1
3	530	3.3	1.9	199	2.0	1.2	20	0	1
6	1310	5.4	2.2	189	2.1	0.8	20	0	1
6	1310	5.4	2.2	209	2.2	0.9	19	0	1
6	1480	5.6	2.3	236	2.2	0.9	19	0	1

Microscopic lesions have been described previously [16]. The lesions and character of the hemorrhage in lung of mice and rabbits were similar regardless of the exposure duration or pressure. Lesions consisted of alveolar hemorrhage composed predominately of cells (erythrocytes and leukocytes) admixed with low to scant quantities of plasma with foci of fibrinogenesis. There were no lesions in the macrovasculature of alveolar septa, terminal airways, bronchioles or in capillaries in connective tissue surrounding bronchioles, or in bronchi.

Four procedures are employed to present the exposure-effect trend results for both the 0.3 dB/cm-MHz derating ($I_{SPPA.3}$, $p_{r.3}$ and *MI*) and at the pleural surface ($I_{SPPA.PS}$, $p_{r.PS}$ and MI_{PS}), *viz.*, column graphs, ANOVA tests, correlation coefficient tests, and linear regression analyses

Fig. 2 graphically shows the mean and standard deviation of the rabbit lung damage score values as functions of $I_{SPPA.3}$, $p_{r.3}$ and *MI*. In Fig. 2(a), the result at $I_{SPPA.3}$ of 200 W/cm^2 is the combined results from the 3 MHz ($MI = 1.3$) and 6 MHz ($MI = 0.8$) listings in Table IV. Likewise, in Fig. 2(c), the result at *MI* of 1.9 is the combined results from the 3 MHz ($I_{SPPA.3} = 420$ W/cm^2) and 6 MHz ($I_{SPPA.3} = 1060$ W/cm^2) listings in Table IV. Prior to combining these groups, the Mann-Whitney U test indicated that the groups that were to be combined were not statistically significantly different.

The Kruskal-Wallis ANOVA test indicates that $I_{SPPA.3}$ (Fig. 2(a)) is considered significant ($p = 0.030$), that $p_{r.3}$ (Fig. 2(b)) is considered significant ($p = 0.045$), and that *MI* (Fig. 2(c)) is considered significant ($p = 0.037$). The Dunn's Multiple Comparisons test did not identify any means which were significantly different for each of the exposure conditions.

The Spearman rank-order nonparametric correlation coefficient test results (Table V) indicate that there is a significant association between each of the exposure quantities ($I_{SPPA.3}$, $p_{r.3}$ and *MI*) and the lung damage score, but there is considerable scatter in the data.

The individual rabbit lung damage score values were subjected to a linear regression analysis as a function of $I_{SPPA.3}$, $p_{r.3}$ and *MI* levels, respectively, and yielded:

$$\text{score} = 0.0006 I_{SPPA.3} + 0.16 \qquad r = 0.49 \quad p = 0.0005 \quad n = 47 \tag{5}$$

$$\text{score} = 0.17 p_{r.3} - 0.044 \qquad r = 0.50 \quad p = 0.0003 \quad n = 47 \tag{6}$$

$$\text{score} = 0.38 MI - 0.067 \qquad r = 0.49 \quad p = 0.0004 \quad n = 47 \tag{7}$$

The run test for all three linear regressions indicated that there was not a significant departure from linearity.

The estimated *in situ* exposure levels at the pleural surface (see (2)–(4)) resulted in a range of values because the distance between the animal's skin surface and pleural surface was variable (see Table IV). Therefore, each exposure quantity was uniformly grouped into six ranges (along with the sham exposure group); six ranges were selected because that was the more common number of groups for the $I_{SPPA.3}$, $p_{r.3}$ and *MI* exposure quantities (see Fig. 2). $I_{SPPA.PS}$ ranged from 52 to 498 W/cm^2, $p_{r.PS}$ from 1.02 to 3.33 MPa and MI_{PS} from 0.41 to 1.45. The mean and standard deviation of the the rabbit lung damage score values

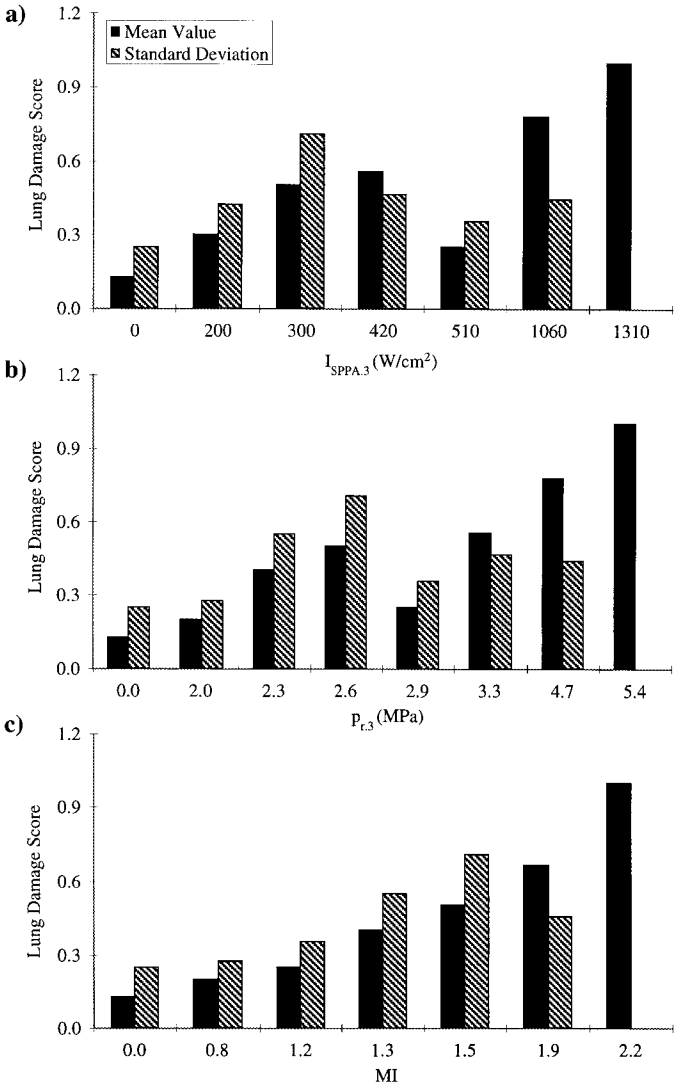

Fig. 2. Mean and standard deviation values of the rabbit lung damage score as a function of (a) derated spatial peak, pulse average intensity ($I_{\mathrm{SPPA.3}}$); (b) derated peak rarefactional pressure ($p_{\mathrm{r.3}}$); and (c) Mechanical Index (MI). Where the standard deviation appears to be missing, the lung damage score valueswere all the same, thus yielding a standard deviation of zero.

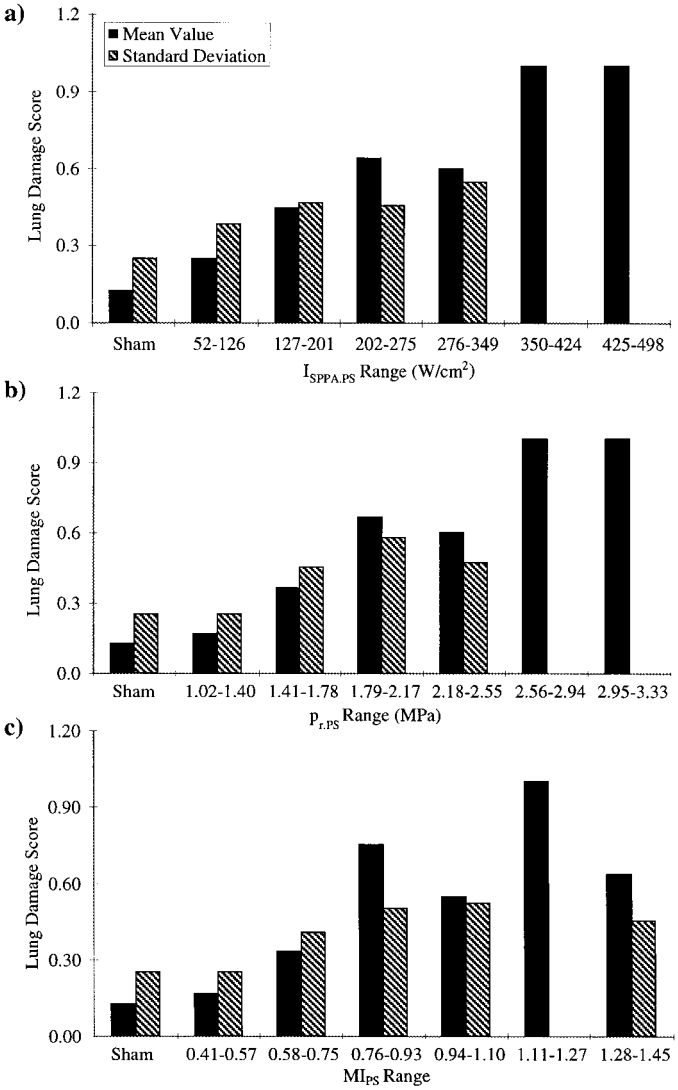

Fig. 3. Mean and standard deviation values of the rabbit lung damage score as a function of ranges of (a) spatial peak, pulse average intensity at the pleural surface ($I_{\mathrm{SPPA.PS}}$), (b) peak rarefactional pressure at the pleural surface ($p_{\mathrm{r.PS}}$), and (c) Mechanical Index at the pleural surface (MI_{PS}). Where the standard deviation appears to be missing, the lung damage score values were all the same thus yielding a standard deviation of zero.

as a function of $I_{\mathrm{SPPA.PS}}$, $p_{\mathrm{r.PS}}$ and MI_{PS} are graphically represented by groups in Fig. 3.

For the seven rabbit exposure groups for each of the estimated *in situ* exposure conditions, the Kruskal-Wallis ANOVA test indicates that $I_{\mathrm{SPPA.PS}}$ (Fig. 3(a)) is considered not quite significant ($p = 0.052$), that $p_{\mathrm{r.PS}}$ (Fig. 3(b)) is considered significant ($p = 0.010$), and that MI_{PS} (Fig. 3(c)) is considered significant ($p = 0.005$). The Dunn's Multiple Comparisons test did not identify any means which were significantly different for each of the exposure conditions.

The Spearman rank-order nonparametric correlation coefficient test results (Table V) indicate that there is a significant association between each of the exposure quantities ($I_{\mathrm{SPPA.PS}}$, $p_{\mathrm{r.PS}}$ and MI_{PS}) and the lung damage score, but there is considerable scatter in the data.

TABLE V
SUMMARY OF THE SPEARMAN RANK-ORDERED CORRELATION COEFFICIENT r_S RESULTS FOR THE 47 RABBIT LUNG DAMAGE SCORE VALUES FOR THE INDICATED EXPOSURE QUANTITIES.

Exposure Quantities	r_S	p value	95% Confidence Interval
$I_{\mathrm{SPPA.3}}$	0.41	0.0047	0.13 to 0.63
$p_{\mathrm{r.3}}$	0.51	0.0003	0.25 to 0.70
MI	0.53	0.0001	0.28 to 0.71
$I_{\mathrm{SPPA.PS}}$	0.50	0.0003	0.24 to 0.69
$p_{\mathrm{r.PS}}$	0.49	0.0004	0.23 to 0.69
MI_{PS}	0.42	0.0037	0.14 to 0.63

The individual rabbit lung damage score values were subjected to a linear regression analysis as a function of $I_{\mathrm{SPPA.PS}}$, $p_{\mathrm{r.PS}}$ and MI_{PS} levels, respectively, and yielded:

$$\text{score} = 0.0020 I_{\mathrm{SPPA.PS}} + 0.11 \qquad r = 0.52 \quad p = 0.0002 \quad n = 47 \quad (8)$$

$$\text{score} = 0.29 p_{\mathrm{r.PS}} - 0.055 \qquad r = 0.51 \quad p = 0.0003 \quad n = 47 \quad (9)$$

$$\text{score} = 0.48 MI_{\mathrm{PS}} - 0.053 \qquad r = 0.43 \quad p = 0.0024 \quad n = 47 \quad (10)$$

The run test for all three linear regressions indicated that there was not a significant departure from linearity.

Of the 43 exposed rabbits, the mean ± standard deviation distance between the skin and pleural surface was 13±1.7 mm (minimum, 9.6 mm; maximum, 16 mm). Using the minimum and maximum distances, at 3 MHz, $I_{\mathrm{SPPA.PS}}$ ranged from 46 to 59% that of $I_{\mathrm{SPPA.3}}$, and $p_{\mathrm{r.PS}}$ and MI_{PS} ranged from 68 to 78% that of $p_{\mathrm{r.3}}$ and *MI*; at 6 MHz, $I_{\mathrm{SPPA.PS}}$ ranged from 21 to 40% that of $I_{\mathrm{SPPA.3}}$, and $p_{\mathrm{r.PS}}$ and MI_{PS} ranged from 46 to 64% that of $p_{\mathrm{r.3}}$ and *MI*. Of the six pigs, the mean ± standard deviation distance between the skin and pleural surface was 21 ± 2.0 mm (minimum, 19 mm; maximum, 24 mm). Using the minimum and maximum distances, at 3 MHz, $I_{\mathrm{SPPA.PS}}$ ranged from 31 to 37% that of $I_{\mathrm{SPPA.3}}$, and $p_{\mathrm{r.PS}}$ and MI_{PS} ranged from 56 to 61% that of $p_{\mathrm{r.3}}$ and *MI*; at 6 MHz, $I_{\mathrm{SPPA.PS}}$ ranged from 14 to 16% that of $I_{\mathrm{SPPA.3}}$, and $p_{\mathrm{r.PS}}$ and MI_{PS} ranged from 38 to 40% that of $p_{\mathrm{r.3}}$ and *MI*. Of the three mice, each had a distance between the skin and pleural surface of 2.0 mm. At 6 MHz, $I_{\mathrm{SPPA.PS}}$ was 82% that of $I_{\mathrm{SPPA.3}}$, and $p_{\mathrm{r.PS}}$ and MI_{PS} were 90% that of $p_{\mathrm{r.3}}$ and *MI*.

VIII. Discussion

One of the purposes of the Output Display Standard's Mechanical Index is to provide an indicator for the potential for producing cavitation *in vivo*. In this study, a specific ultrasonically induced biological effect, *viz.*, lung hemorrhage, is being used to evaluate the Mechanical Index as an indication. It needs to be emphasized, however, that there has been no reported instance where diagnostic ultrasound has been shown to produce either cavitation or lung hemorrhage in patients.

For each frequency individually (see Table IV), the mean rabbit lung damage score values increased as a function of each of the three exposure quantities, *viz.*, $I_{\mathrm{SPPA.3}}$, $p_{\mathrm{r.3}}$, and *MI*. This provides support that the superthreshold experimental design is responding as anticipated, that is, an increase in the degree of a biologic effect when the acoustic pressure level is the only variable increased. Thus, at a specific center frequency, any one of the three exposure quantities could be used as an exposure-effect index for providing guidance to equipment users of a nonthermal bioeffect risk, at least based on lung damage. However, center frequency is a necessary variable to consider because a range of frequencies is routinely used clinically. The Mechanical Index was developed to take into consideration center frequency.

The *MI* appears to be a better indicator of rabbit lung damage than either the $I_{\mathrm{SPPA.3}}$ or $p_{\mathrm{r.3}}$ as assessed graphically (Fig. 2) from the mean lung damage score values. The graphical representation shows a dip in the mean lung damage score value at 510 W/cm^2 (Fig. 2(a)) and at 2.9 MPa (Fig. 2(b)), both representing the same group of 10 rabbits at one of the 6 MHz exposure conditions. However, this same group of 10 rabbits has an *MI* of 1.2 (Fig. 2(c)) for which no dip is observed in the mean lung damage score value. Admittedly, this is a single exposure condition which one might argue is anomolous. Until this class of experiments is repeated (not only with lung damage but also with some other nonthermal bioeffect) using a wider range of frequencies, this possible concern cannot be addressed.

The Searman correlation coefficient (Table V) suggests that the *MI* and $p_{\mathrm{r.3}}$ are better indicators (lower p values) of rabbit lung damage than the $I_{\mathrm{SPPA.3}}$, but considerable spread in the lung damage scores is evident from the values of r_{S}. Also, all three exposure quantities appear to be equivalent indicators (essentially the same p values) of lung damage as assessed *via* regression analysis (5)–(7), but, here again, considerable spread in the lung damage scores is evident from the values of r. The spread in the lung damage scores results because significant lung damage was not produced, and the lung damage score values were at the low end of the scoring criteria, that is, only 0, 0.5, and 1.

In summary, the *MI* appears to be an either equivalent (as assessed *via* regression analysis) or better (as assessed graphically and by the Spearman correlation coefficient) predictor of lung hemorrage in rabbits than $I_{\mathrm{SPPA.3}}$.

In principal, the *in situ* exposure should be a better indicator of the rabbit lung damage score and, thus, provide the basis for a better understanding of the physical mechanism responsible for the ultrasonically induced damage. There is a dearth of ultrasonic propagation property data of the region between the thoracic (ventral, lateral, or dorsal) and the pleural surfaces. Measured attenuation at 1.1 and 3.4 MHz in 7-week-old mice was 1.5 to 5.2 dB and 2.5 to 6.9 dB [1], [18], and assuming a thickness of 2 mm (see Table IV) yields attenuation coefficients of 6.8 to 24 and 3.7 to 10 dB/cm-MHz, respectively, which seem too high. Estimated attenuation coefficient at 2.3 MHz in 1-2-day-old crossbred pigs was 1.1 to 1.3 dB/cm-MHz [19]. Therefore, a correction to the 0.3 dB/cm-MHz derating factor of 1 dB/cm-MHz to estimate the *in situ* exposure levels at the pleural surface was assumed and based on striated muscle attenuation coefficient values [17].

None of the *in situ* estimated exposure conditions appears to be a better exposure-effect quantity as assessed graphically (Fig. 3) for tracking lung hemorrhage. The Searman correlation coefficient (Table V) and the linear regression analysis (8)–(10) suggest that the $I_{\mathrm{SPPA.PS}}$ and $p_{\mathrm{r.PS}}$ are better indicators (lower p values) of rabbit lung

damage than the MI_{PS}, but considerable spread in the lung damage scores is evident from the values of r_S and r, respectively, with the greatest spread noted for MI_{PS}.

Comparison of the 0.3 dB/cm-MHz ODS derated lung hemorrhage results with the 1 dB/cm-MHz *in situ* estimated results suggests that there is essentially no difference for I_{SPPA} and p_r exposure quantities. However, the *MI* is tracked slightly better than the MI_{PS}.

It is, therefore, suggested that the 0.3 dB/cm-MHz ODS *MI* is at least equivalent to the other five exposure quantities evaluated ($I_{SPPA.3}$, $p_{r.3}$, $I_{SPPA.PS}$, $p_{r.PS}$, MI_{PS}) as an exposure-effect quantity for tracking rabbit lung hemorrhage at superthreshold exposure conditions, and may even be slightly better in some cases. The scope of this study is insufficient to provide a more definitive conclusion.

As compared to clinical signs caused by continous-wave 30 kHz ultrasound [20]–[22], pulsed-wave ultrasound caused no abnormalities in respiratory rates or breathing patterns in species exposed. The differences in clinical effects can be explained, in part, by the greater extent and degree of injury caused by exposure to continuous-wave ultrasound at 30 kHz when compared to pulsed-wave ultrasound at 3 and 6 MHz.

The six pig lung exposures did not exhibit any observable damage at either 3 or 6 MHz. For the 0.3 dB/cm-MHz ODS exposure conditions, the pig exposure levels ($I_{SPPA.3}$, $p_{r.3}$, and *MI*) were as high or higher than the rabbit exposure levels at each frequency, levels which produced lung damage in rabbits whereas, for the *in situ* estimated exposure conditions, the pig exposure levels ($I_{SPPA.PS}$, $p_{r.PS}$, and MI_{PS}) were within the range of the rabbit exposure levels at each frequency between adult rabbits and pigs. The three mouse exposures produced greater lung damage than comparable rabbit exposure levels. The 0.3 dB/cm-MHz ODS exposure levels ($I_{SPPA.3}$, $p_{r.3}$, and *MI*) for the mice were at the higher end but within the exposure range of the rabbit exposure conditions whereas, for the *in situ* estimated exposure conditions, the mouse exposure levels ($I_{SPPA.PS}$, $p_{r.PS}$, and MI_{PS}) were as high or higher than the rabbit exposure levels. Thus, a species-dependent effect is suggested from these observations, particularly between adult rabbits and pigs.

Other studies support the suggestion of a species-dependent effect. Significant species-dependent effects between 24 mice and 16 rabbits [21] and between 18 mice, 75 rabbits, and 74 pigs [22] have been previously reported using continuous-wave exposure conditions at an ultrasonic frequency of 30 kHz. In the former study [21], using exactly the same superthreshold exposure conditions and lung assessment criteria, it appeared that the adult mouse lung was more sensitive to ultrasound-induced hemorrhage than that of the adult rabbit. Likewise, for the latter study [22], under the same superthreshold exposure conditions and lung assessment criteria, the adult mouse lung was determined to be more sensitive to ultrasound-induced damage than that of the adult rabbit, and the adult rabbit lung was more sensitive to ultrasound-induced damage than that of the adult pig. However, lung damage in 1- 2-day-old Crossbred pigs showed an ultrasound-induced threshold value comparable to that of the mouse [19], thus suggesting that there may not be a species-dependent difference.

Macroscopic lesions also reflected biological differences in lung responses to the two wave forms as well as the physical differences in the source transducers. Pulsed-wave ultrasound and its restricted beam width caused focal hemorrhage with contiguous hemorrhage in subjacent parenchyma; the wider beam width associated with continuous-wave ultrasound caused wide spread hemorrhage and associated injury [16]. It is plausible to speculate that the susceptibility to ultrasound-induced lung hemorrhage may be determined by the thickness of the chest wall or visceral pleura (protective attenuation layers) and that lung tissue of all species responds in the same manner to ultrasound. A second explanation for species differences in the extent and severity of lung hemorrhage induced by ultrasound may be a direct reflection of structural, functional, and physiological differences (pig > rabbit > mouse) in innate mechanical properties such as alveolar surface area (including alveolar diameter), thickness of alveolar septa, lung compliance, and pleural thickness [16], [22]. Although the relationships between mechanical properties of lung tissue and the cause of lung hemorrhage following exposure to continuous and pulsed wave ultrasound are poorly understood, it is likely that the mechanical properties discussed above are important variables in determining the ability of lung to respond to and recover from ultrasound exposure.

Microscopically, hemorrhage and lesions induced by both wave forms were similar [16]; however, there were some variations in the lesion character (ratio of number of cells to volume of plasma, degree of fibrinogenesis affecting the plasma, degree of alveolar septal damage) that could potentially reflect differences in wave form interaction with biological tissues at the cellular or subcellular level. Microscopic evaluation failed to demonstrate lesions in the macrovasculature that could explain a pathogenesis for the hemorrhage thus suggesting that hemorrhage arose from injury to alveolar septa, specifically the microvasculature [16]. Initially, microvascular injury could be associated with alterations or permeability changes at intracellular junctions (tight junctions) of endothelial cells within septa or through direct effects on cell strucuture (cell membranes) or organelles (cell junctions) within endothelial cells. Although the mechanism of injury associated with wave interactions and biological tissue is speculative, we have observed differences in the ratio of cell numbers to plasma volume and the occurrence of alveolar septal necrosis between animals exposed to CW versus pulsed ultrasound [16]. Each wave form (CW versus pulsed) could have different biological effects, either directly (mechanical) or indirectly (cavitation-like) on endothelial cells forming the microvasculature. Such injury would likely occur through interactions with celluar structures such as cell membrane systems (lipid or protein interactions) and at endothelial cell junctions early in the genesis of the lesions.

A second plausible mechanism for microvascular injury could result from simple physical or mechanical trauma (laceration or tearing) caused by ultrasound (a deformation response) or by more complicated mechanisms related to cavitation-like phenomena [9], [23]. Physical injury such as tearing or laceration may be associated with direct mechanical effects of ultrasound on pleural surfaces and avleolar septa. This hypothesis is supported by the observation that hemorrhage occurs as early as one minute after exposure to continuous wave ultrasound (J. F. Zachary, private communication, May, 1993). The cavitation-like phenomenon, which could have physical and biological effects, describes the rapid collapse and expansion of air bubbles (less than 10 μm in diameter) associated with ultrasound-bubble interaction. This process results, *in vitro*, in the eventual destruction of the bubble and release of air from the bubble (jet formation possibly) which is at an extremely high temperature and pressure [26]. Cavitation also results in enlargement of existing bubbles through fusion with smaller bubbles (coalescence). The effects of cavitation phenomena have yet to be proven, *in vivo*, but theoretically, the expansion of larger air bubbles in alveoli could exceed the ability of associated structures (septa, pleura) to respond to and recover from bubble expansion resulting in physical or mechanical injury to these structures with subsequent hemorrhage.

A thermal mechanism is not considered plausible for either the 3- and 6-MHz results reported herein, or for the 30-kHz results reported previously [20]–[22]. Previously, estimated axial temperature increase profiles were calculated for an ATL HDI® UM9 diagnostic ultrasound system operating in triple mode under conditions similar to those used herein; the steady-state maximum temperature increase was about 0.5°C [24]. Also, applying the monopole-source solution for estimating tissue temperature increases [25] for the 30-kHz field, the steady-state maximum temperature increase was about 0.1°C (attenuation and absorption coefficient = 1 dB/cm-MHz, perfusion length = 1 cm, source diameter = 8 cm, unfocused, acoustic pressure amplitude = 145 kPa).

Hemorrhage occurred in areas of lung closest to the pulsed-ultrasound beam and were located under the intercostal space. Each focus of hemorrhage, independent of its size, appeared directly related to a pleural surface suggesting the mechanism of injury resulting in hemorrhage was initiated at the pleural surface and then spread into lung parenchyma. This finding is important because, in theory, sound waves do not readily pass into lung tissues because of its low impedance (air filled) relative to the adjacent tissue. In order to produce lung hemorrhage within lung parenchyma, a means would have to develop to propagate and spread sound waves through lung tissue. It is likely that the initial focus of hemorrhage is in the pleura and contiguous alveoli. Septal damage and resultant hemorrhage into alveoli displaces air and fills alveoli with plasma and cells, an ideal medium for sound waves to spread and induce lesions in unaffected alveolar septa. This mechanism could propagate lesions continually in species with anatomic and physiologic properties of lung tissue such as those that exist in mice when compared to other species phylogenetically closer to human beings [16], [21], [27]–[33]. This mechanism also may have limited biological significance in species with anatomic and physiologic properties of lung tissue that could minimize the extent and degree of injury to mechanical or biological injury. In support of this latter hypothesis, structural and functional differences exist in lung compliance, septal thickness, alveolar diameter, and septal deposition of collagen fibers as examples between mice, rabbits, and pigs [16], [21], [27]–[33]. This mechanism is unproven but these structural differences are likely to be very important in determining lung responses to injury.

Even though ultrasound cannot readily pass into air-filled alveoli, air-filled alveoli are required for the induction of lung hemorrhage by ultrasound [11]; hemorrhage is not produced in fetal lung exposed to ultrasound *in utero*, whereas hemorrhage is produced by ultrasound in neonatal aerated lung.

Species differences in reponses to ultrasound may be a reflection of structural, functional, and physiological differences in innate mechanical properties such as alveolar surface area, diameter, or volume; thickness of alveolar septa; lung compliance; and pleural thickness (see compilations in [20]–[21] and also [27]–[33]).

Tissue attenuation between the skin and pleural surface is unlikely to play a role in determining a species sensitivity to ultrasound. The derated (at 0.3 dB/cm-MHz) exposure quantities are an overestimate of the exposure quantities at the pleural surface since the tissue attenuation of the interposed tissue between the skin surface and pleural surface is assumed to be greater than this derating factor. A correction to the 0.3 dB/cm-MHz derating factor was used ((2)–(4)) to estimate the *in situ* exposure levels at the pleural surface for each of the animals by assuming an attenuation coefficient of 1 dB/cm-MHz which was estimated from striated muscle attenuation coefficient values [17].

Finally, all these observations are under superthreshold exposure conditions; they are not threshold studies. It cannot be assessed from these studies whether there is a species-dependent effect on the threshold of lung damage. Additionally, all species are adults. These studies need to be extended to the examination of age dependencies since the morphological characteristics of lung change with age.

In summary, using the mechanical biophysical index as defined in the Output Display Standard [3], the Mechanical Index is, at least, an equivalent, and in some cases, may be a better indicator of nonthermal bioeffect risk than the derated spatial peak, pulse average intensity. Further, this study, combined with two previous studies [21]–[22] suggest a species-dependent effect of ultrasound-induced lung damage under superthreshold exposure conditions.

Acknowledgments

The authors gratefully acknowledge the technical support from Larry Grove of Advanced Technology Laboratories, and Henri C. Bianucci, Nadine Barrie Smith, and Darshan Gandhi of the University of Illinois.

References

[1] S. Z. Child, C. L. Hartman, L. A. Schery, and E. L. Carstensen, "Lung damage from exposure to pulsed ultrasound," *Ultrasound Med. Biol.*, vol. 16, pp. 817–825, 1990.

[2] "Guide for measuring and reporting acoustic output of diagnostic ultrasound medical devices, Document 510(k)," Center for Devices and Radiological Health, Food and Drug Administration, US Depart. Health Human Services, Rockville, MD, 1985.

[3] *Standard for Real-Time Display of Thermal and Mechanical Indices on Diagnostic Ultrasound Equipment*, AIUM Publications, American Institute of Ultrasound in Medicine, Laurel, MD 20707.

[4] "Revised 510(k) diagnostic ultrasound guidance for 1993," Center for Devices and Radiological Health, Food and Drug Admin., US Depart. Health Human Services, Rockville, MD, February 17, 1993.

[5] "Use of mechanical index in place of spatial peak, pulse average intensity in determining substantial equivalence," Center for Devices and Radiological Health, Food and Drug Admin., US Depart. Health Human Services, Rockville, MD, April 14, 1994.

[6] *Implementation of the Principle of As Low As Reasonably Achievable (ALARA) for Medical and Dental Personnel*, National Council on Radiation Protection and Measurement, Bethesda, MD, Rep. No. 107, December 31, 1990.

[7] *Exposure Criteria for Medical Diagnostic Ultrasound: I. Criteria Based on Thermal Mechanisms*, National Council on Radiation Protection and Measurement, Bethesda, MD, Rep. No. 113, June 1, 1992.

[8] "World Federation for Ultrasound in Medicine and Biology symposium on safety and standardization in medical ultrasound: Issues and recommendations regarding thermal mechanisms for biological effects of ultrasound," *Ultrasound Med Biol.*, vol. 18, pp. 731–814 1992.

[9] R. E. Apfel and C. K. Holland, "Gauging the likelihood of cavitation from short pulse, low duty cycle diagnostic ultrasound," *Ultrasound Med. Biol.*, vol. 17, pp. 179–188, 1991.

[10] C. K. Holland and R. E. Apfel, "An improved theory for the prediction of microcavitation thresholds," *IEEE Trans. Ultrason., Ferroelect., Freq. Contr.*, vol. 36, pp. 204–208, 1989.

[11] C. Hartman, S. Z. Child, R. Mayer, and E. L. Carstensen, "Lung damage from exposure to the fields of an electrohydraulic lithotripter," *Ultrasound Med. Biol.*, vol. 16, pp. 675–679, 1990.

[12] C. K. Holland and R. E. Apfel, "Thresholds for transient caviation produced by pulsed ultrasound in a controlled nuclei environment," *J. Acoust. Soc. Amer.*, vol. 88, pp. 2059–2069, 1990.

[13] C. K. Holland, R. A. Roy, R. E. Apfel, and L. A Crum "*In vitro* detection of cavitation induced by a diagnostic ultrasound system," *IEEE Trans. Ultrason., Ferroelect., Freq. Contr.*, vol. 39, pp. 95–101, 1992.

[14] M. L. Cook, *The Anatomy of the Laboratory Mouse*, New York: Academic, 1965.

[15] P. Popesko, *Atlas of Topographical Anatomy of the Domestic Animals*, vol. 2, Philadelphia: Saunders, 1977.

[16] J. F. Zachary and W. D. O'Brien, Jr., "Lung hemorrhage induced by continuous and pulsed wave (diagnostic) ultrasound in mice, rabbits, and pigs," *Vet. Pathol.*, vol. 32, pp. 43–54, 1995.

[17] *Biological Effects of Ultrasound: Mechanisms and Clinical Implications*, National Council on Radiation Protection and Measurement, Bethesda, MD, Rep. No. 74, December 30, 1983.

[18] C. H. Raeman, S. Z. Child, and E. L. Carstensen, "Timing of exposures in ultrasonic hemorrhage of murine lung," *Ultrasound Med. Biol.*, vol. 19, pp. 507–512, 1993.

[19] R. Baggs, D. P. Penney, C. Cox, S. Z. Child, C. H. Raeman, D. Dalecki and E. L. Carstensen, "Thresholds for ultrasonically induced lung hemorrhage in neonatal swine," *Ultrasound Med. Biol.*, vol. 22, pp. 119–128, 1996.

[20] W. D. O'Brien, Jr., and J. F. Zachary, "Mouse lung damage from exposure to 30 kHz ultrasound," *Ultrasound Med. Biol.*, vol. 20, pp. 287–297, 1994.

[21] W. D. O'Brien, Jr., and J. F. Zachary, "Comparison of mouse and rabbit lung damage exposure to 30 kHz ultrasound," *Ultrasound Med. Biol.*, vol. 20, pp. 299–307, 1994.

[22] W. D. O'Brien, Jr., and J. F. Zachary, "Rabbit and pig lung damage comparison from exposure to continuous wave 30-kHz ultrasound," *Ultrasound Med. Biol.*, vol. 22, pp. 345–353, 1996.

[23] G. ter Haar, "Ultrasonic biophysics," in *Physical Principles of Medical Ultrasonics*, C. R. Hill, Ed., New York: Wiley, 1986, pp. 388–408.

[24] A. F. Tarantal, S. E. Gargosky, D. S. Ellis, W. D. O'Brien, Jr., and A. G. Hendrickx, "Hemotologic and growth-related effects of frequent prenatal ultrasound exposure in the long-tailed macaque (Macaca fascicularis)," *Ultrasound Med. Biol.*, vol. 21, pp. 1073–1081, 1995.

[25] D. S. Ellis and W. D. O'Brien, Jr., "The monopole-source solution for estimating tissue temperature increases for focused ultrasound fields," *IEEE Trans. Ultrason., Ferroelect., Freq. Contr.*, vol. 43, pp. 88–97, 1996.

[26] T. J. Mason and J. P. Lorimer, *Sonochemistry: Theory, Applications and Uses of Ultrasound in Chemistry*, New York: Wiley, 1988.

[27] R. R. Mercer and J. D. Crapo, "Architecture of the acinus," in *Comparative Biology of the Normal Lung*, R. A. Parent, Ed., Boca Raton: FL: CRC Press, 1992. Ch. 10, pp. 109–119.

[28] K. E. Pinkerton, P. Gehr, and J. D. Crapo, "Architecture and cellular composition of the air-blood barrier," in *Comparative Biology of the Normal Lung*, R. A. Parent, Ed., Boca Raton: FL: CRC Press, 1992. Ch. 11, pp. 121–128.

[29] H. Sahebjhami, "Aging of the normal lung," in *Comparative Biology of the Normal Lung*, R. A. Parent, Ed., Boca Raton: FL: CRC Press, 1992. Ch. 21, pp. 351–366.

[30] S. M. Tenney and J. E. Remmers, "Comparative quantitative morphology of the mammalian lung: diffusing area, *Nature*, vol. 197, pp. 54–56, 1963.

[31] W. S. Tyler and M. D. Julian, "Gross and subgross anatomy of lungs, pleura, connective tissue septa, distal airways, and structural units," in *Comparative Biology of the Normal Lung*, R. A. Parent, Ed., Boca Raton: FL: CRC Press, 1992. Ch. 4, pp. 37–47.

[32] J. W. Watson, "Elastic, resistive, and inertial properties of the lung," in *Comparative Biology of the Normal Lung*, R. A. Parent, Ed., Boca Raton: FL: CRC Press, 1992. Ch. 16, pp. 175–216.

[33] E. R. Weibel, "Dimensions of the tracheobronchial tree and alveoli," in *Biological Handbooks: Respiration and Circulation*, P. L. Altman and D. S. Dittmer, Eds., Bethedsa, MD: Federation Amer. Soc. Exper. Biol., 1971. Ch. 51.

William D. O'Brien, Jr. (S'64–M'71–SM'79–F'89) received B.S., M.S., and Ph.D. degrees in 1966, 1968, and 1970, from the University of Illinois, Urbana-Champaign.

From 1971 to 1975 he worked with the Bureau of Radiological Health (currently the Center for Devices and Radiological Health) of the U.S. Food and Drug Administration. Since 1975, he has been at the University of Illinois, where he is a Professor of Electrical and Computer Engineering and of Bioengineering, College of Engineering, and Professor of Bioengineering, College of Medicine, is the Director of the Bioacoustics Research Laboratory and is the Program Director of the NIH Radiation Biophysics and Bioengineering in Oncology Training Program. His research interests involve the many areas of ultrasound-tissue interaction, including spectroscopy, risk assessment, biological effects, tissue characterization, dosimetry, blood-flow measurements, acoustic microscopy and meat characterization for which he has published more than 170 papers.

Dr. O'Brien is Editor-in-Chief of the *IEEE Transactions on Ultrasonics, Ferroelectrics, and Frequency Control*. He is a Fellow of the Institute of Electrical and Electronics Engineers (IEEE), the Acoustical Society of America (ASA), and the American Institute of Ultrasound in Medicine (AIUM) and a Founding Fellow of the American Institute of Medical and Biological Engineering. He was recipient of the IEEE Centennial Medal (1984), the AIUM Presidential Recognition Awards (1985 and 1992), the AIUM/WFUMB Pioneer Award (1988), the IEEE Outstanding Student Branch Counselor Award (1989), and the AIUM Joseph H. Holmes Basic Science Pioneer Award (1993). He has been President (1982–1983) of the IEEE Sonics and Ultrasonics Group (currently the IEEE UFFC-Society), Co-Chairman of the 1981 IEEE Ultrasonic Symposium, and General Chairman of the 1988 IEEE Ultrasonics Symposium. He has also been President of the AIUM (1988–1991) and Treasurer of the World Federation for Ultrasound in Medicine and Biology (1991–1994).

James F. Zachary received a B.S. degree from Northern Illinois University, Dekalb, in 1972 and D.V.M. and Ph.D. degrees in 1977 and 1983, from the University of Illinois, Urbana-Champaign.

From 1978, he has been at the University of Illinois, where he is an Associate Professor of Pathology. His research interests involve ultrasound-tissue interaction and include biological effects, tissue characterization, blood-flow measurements, and acoustic microscopy. He also studies the role of microglial cells, astrocytes, and brain cytokines in neurodegenerative diseases. He has published more than 50 papers.

Dr. Zachary is Editor-in-Chief of *Veterinary Pathology*. He is a Diplomate in the American College of Veterinary Pathologists and a member of the American Institute of Ultrasound in Medicine (AIUM) and its Bioeffects Committee, the American Society for Investigative Pathology (FASEB), and the Society for Neuroscience.